

ZrTiO₄ Nanowire Growth Using Membrane-assisted Pechini Route

Poty Rodrigues de Lucena^{a*}, Willian Andrade Prado^b, Valdeilson Souza Braga^a, Neftali Lenin Villarreal Carreño^c

^aUniversidade Federal do Oeste da Bahia, Centro de Ciências Exatas e das Tecnologias - CCET, Rua Professor José Seabra de Lemos, 316, Recanto dos Pássaros, CEP 47.805-028, Barreiras, Bahia, Brazil.

^bUniversidade Federal do Rio Grande do Sul - R. Sarmento Leite, 245 - Centro Histórico, Porto Alegre - RS, 90050-170, Brazil.

^cUniversidade Federal de Pelotas, Novonano - Grupo de Tecnologias Aplicadas de Materiais Avançados. R. Gen. Osório, 725 - Centro, Pelotas - RS, 96020-000, Brazil.

Article history: Received: 02 March 2015; revised: 02 October 2015; accepted: 06 October 2015. Available online: 07 February 2016. DOI: <http://dx.doi.org/10.17807/orbital.v1i1.711>

Abstract: The high surface-to-volume ratio of nanowires makes them natural competitors as newer device components. In this regard, a current major challenge is to produce quasi-one-dimensional nanostructures composed of well-established oxide-based materials. This article reports the synthesis of ZrTiO₄ nanowires on a silicon (100) wafer in a single-step deposition/thermal treatment. The template-directed membrane synthesis strategy was associated with the Pechini route and spin-coating deposition technique. ZrTiO₄ nanowires were obtained at 700 °C with diameters in the range of 80-100 nm. FEGSEM images were obtained to investigate ZrTiO₄ nanowire formation on the silicon surface and energy dispersive X-ray detection (EDS) and X-ray diffraction (XRD) analyses were performed to confirm the oxide composition and structure.

Keywords: template-synthesis; ZrTiO₄; nanowire; Pechini method.

1. INTRODUCTION

The current revolution in the area of new electronic materials suggests that graphene, conductive polymers, and metal oxides are the protagonists. However, the construction of 3D arrays of conventional 1D nanomaterials, such as nanorods and nanowires in general, and their large-scale integration on amorphous silicon (a-Si) and polycrystalline silicon (poly Si) remain crucial challenges associated with the very promising future of the application of nanotechnology to a range of areas including field-effect transistors, gas sensors, and solar cells [1, 2].

A worldwide effort to develop soft-chemistry synthesis strategies is underway to produce a variety of semiconductor and oxide nanostructures [3]. Many techniques have been developed along with a significantly enhanced fundamental understanding and thus the field is evolving rapidly with new synthetic methods and new nanowires or nanorods

being reported in the literature [4]. In particular, template-based synthesis is a common approach used to grow conventional nanorods, nanowires, nanotubes and new 1D nanomaterials [5 - 7].

The Pechini method has been used extensively in the synthesis of a variety of mono-, bi- and multi-metallic oxides. The experimental simplicity and reproducibility of the methods, combined with the stoichiometric rigor in the synthesis of metal oxide compositions, especially in oxides comprising two or more metals, have increased their field of application to the synthesis of ferroelectric solid-solutions, photoluminescent powders, magnetic materials, superconductors, nanoparticles, and photovoltaic materials. In this synthetic strategy, metallic cations linked to ester chains can be obtained through a condensation between a metal citrate and a hydroxyl alcohol under acid catalytic conditions [8].

Membrane template-based synthesis of oxide nanostructures can be carried out by filling with precursor solutions the nanopores of various

*Corresponding author. E-mail: poty@ufob.edu.br

polymeric or oxide membrane supports [9 - 11], such as cellulose acetate, polycarbonate (PC), PVDF, PTFE and anodized alumina oxide (AAO), and nanomembranes [12]. AAO and PC membranes are conveniently used for the growth of nanostructures from various chemical and/or physical synthetic strategies [13 - 15]. The diameter and length of the nanostructures obtained can be controlled by the pore size and thickness of the template membrane, but elimination of the membrane is dependent on certain experimental conditions. Although oxide nanostructures have been grown by applying chemical methods, the experimental conditions have strongly limited the compositions to monometallic oxides such as ZnO, SnO₂, In₂O₃ or TiO₂. No studies have previously been devoted to the synthesis of ZrTiO₄ oxide nanorods, nanowires, nanotubes or new 1D nanomaterials.

The removal of the AAO (Al₂O₃) template membrane can be conducted by acidic or basic chemical etching. In turn, polycarbonate membranes can be removed by heat treatment at moderate temperatures or dissolution with organic solvents, maintaining the desired oxide composition after removal.

In this study, bimetallic oxide nanowires were prepared using a template-directed method that combines the Pechini process with a spin-coating technique. PC membranes were used as a template to obtain zirconium titanate, ZrTiO₄, with a morphology of nanowire oxide (ZT-nw) integrated into a silicon substrate.

2. MATERIALS AND METHODS

Our strategy to design the morphology of the ZrTiO₄ oxide consisted of the deposition of a metallic precursor solution onto the membrane pores and the growth of the nanostructure materials by thermal treatment on a silicon substrate with the total removal of the template membrane. The chemical route used in this study was the polymeric precursor method, also called the Pechini method. Further details on the synthesis of the ZrTiO₄ oxide precursor solution can be found in a previous study [16]. The viscosity of the solution was previously adjusted to 12.4 mPa by water evaporation and evaluated by coaxial cylinder rheometry (Quimis rheometer). Briefly, 0.1 mL of the precursor solution was deposited with a micropipette on the PC membrane with 100 nm pore diameter and 13 mm external diameter (SPI Supplies). Some

vacuum was applied to the PC membrane aided by a filtration support for 13 mm membranes adapted to a 500 mL filter flask. In the next stage, a spinning process of the impregnated membrane was employed in the spin coater equipment (Laurell, WS-400-6NPP-LITE) at 7,000 RPM for 20 s. The impregnated PC membranes were then attached to Si (100) substrates (Nova Electronics), previously cleaned with a 4:1 v/v H₂SO₄:H₂O₂ solution. The thermal treatment of the impregnated PC membrane attached to the silicon substrate was performed in an electric oven under aerial atmosphere at a heating rate of 5 °C.min⁻¹ in two temperature steps: the first at 350 °C for two hours for the organic matter pyrolysis, and the second at 700 °C for two hours to obtain the nanowire oxide structure definition. A ZrTiO₄ powder sample was obtained with the same precursor solution under identical thermal treatment conditions for crystalline phase comparison. Field emission scanning electron microscopy (FEG-SEM) and energy dispersive X-ray detection (EDS) was performed by direct morphological and microstructural characterization (Jeol, JSM-7500F) of the sample with a silver electrical contact connected to the aluminum microscope support. In order to evaluate the crystalline phase, the ZT-nws in the silicon substrate were analyzed in a Rigaku Ultima IV diffractometer, with CuK_α radiation ($\lambda = 1.5406 \text{ \AA}$), operating at room temperature. The data were collected in the 5-75° 2 θ range, at a constant-step rate of 0.02 2 θ /s.

3. RESULTS AND DISCUSSION

Figure 1 shows the X-ray diffraction (XRD) pattern for the ZT-nws. The XRD analysis reveals the manifestation of peaks that can be associated with a ZrTiO₄ orthorhombic crystal system (JCPDS No: 00-034-0415). Table 1 shows the (*hkl*) diffraction planes and the respective estimated 2 θ Bragg positions for the ZT-nw diffraction planes.

(<i>hkl</i>)	ZT-nws	JCPDS Card
(011)	23.4	24.61
(111)	30.4	30.44
(200)	35.8	35.64
(201)	40.3	40.43
(121)	42.3	41.91
(202)	52.6	52.63
(013)	60.4	60.17
(311)	61.0	61.79

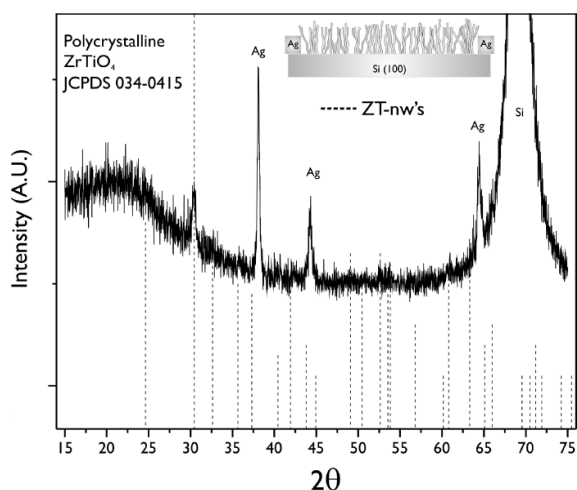


Figure 1. X-ray diffraction of the ZrTiO_4 nanowires deposited on silicon wafer and JCPDS n° 034-0415 peak indexation (dotted lines).

The most intense diffraction peak centered at 30.4° is assigned to the 100% peak of the orthorhombic ZrTiO_4 polycrystalline oxide. Despite the low intensity and presence of noise in the X-ray diffraction profile, some peaks could be assigned to the ZT-nw planes on the silicon wafer. X-ray diffraction data clearly reveals the preferential growth of the ZT-nw's (111) plane in 30.4° . X-ray diffraction (XRD) of the ZrTiO_4 powder obtained from thermal treatment at 700°C of the same precursor polymer deposited on the membranes was performed to confirm the crystalline phase of the final material (Figure 2).

The presence of three sharp peaks at 38.11° , 44.32° and 64.45° are associated with the silver

electrical contact applied to the sample in the FEG-SEM experiments. The broad and intense peak in the $65\text{--}72^\circ$ 2θ range centered at 69° (Figure 1) is related to the silicon wafer. After membrane deposition and thermal treatment steps, the silicon substrate maintained the characteristic shiny finish of the polished surface with minimal tone variation, indicating a good adhesion of the oxide to the substrate.

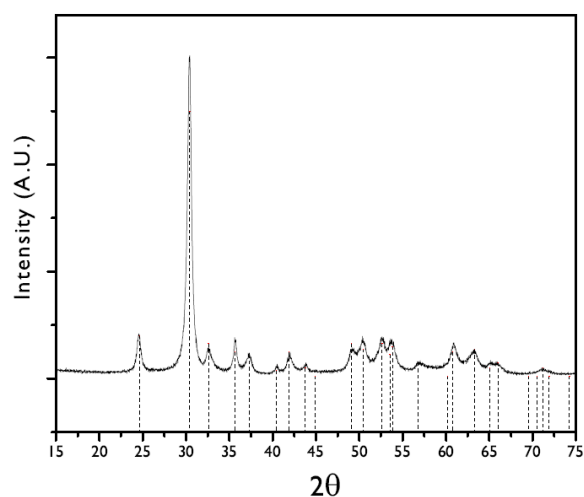
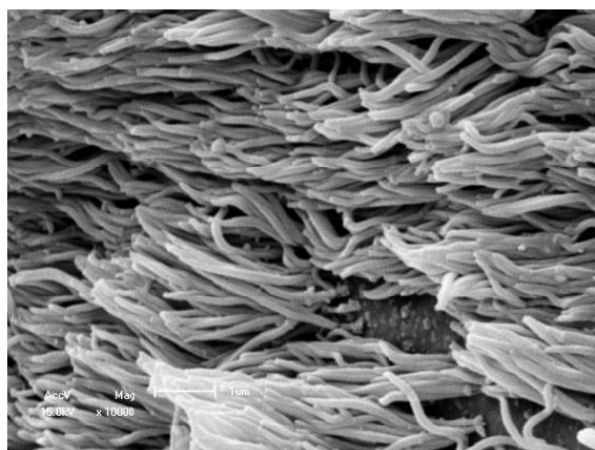
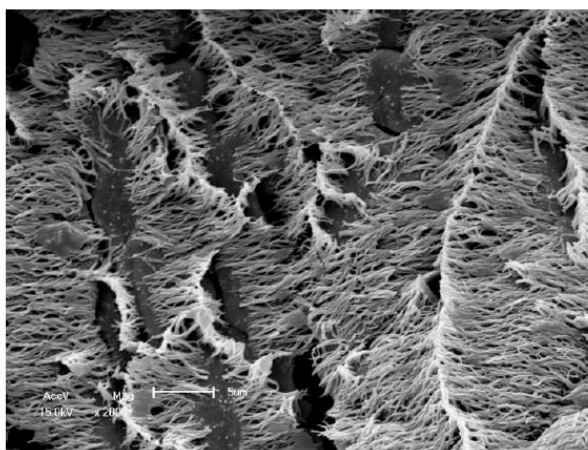


Figure 2. X-ray diffractogram of the ZrTiO_4 powder obtained at 700°C and JCPDS n° 034-0415 peak indexation (dotted lines).

Figures 3 and 4 both show the images of the ZT-nws and a more detailed view of the nanostructures obtained by field emission gun scanning electron microscopy (FEG-SEM). ZrTiO_4 nanowires were formed with a reasonable level of organization, producing highly populated regions of ZT nanostructures.



(a)



(b)

Figure 3. Scanning electron microscopy images of zirconium titanate nanowires on the silicon substrate.

The diameter (d) and length (l) of the nanowires were measured by comparative analysis

with the standard ruler in the electron microscopy images. The nanostructures show a mean aspect ratio (l/d) of approximately 30, with average length and diameter of 2,0 μm and 70 nm, respectively (Figure

4(d)). In some cases, the ZT-nws were joined along their lengths and often at an inclination due to the high aspect ratio value

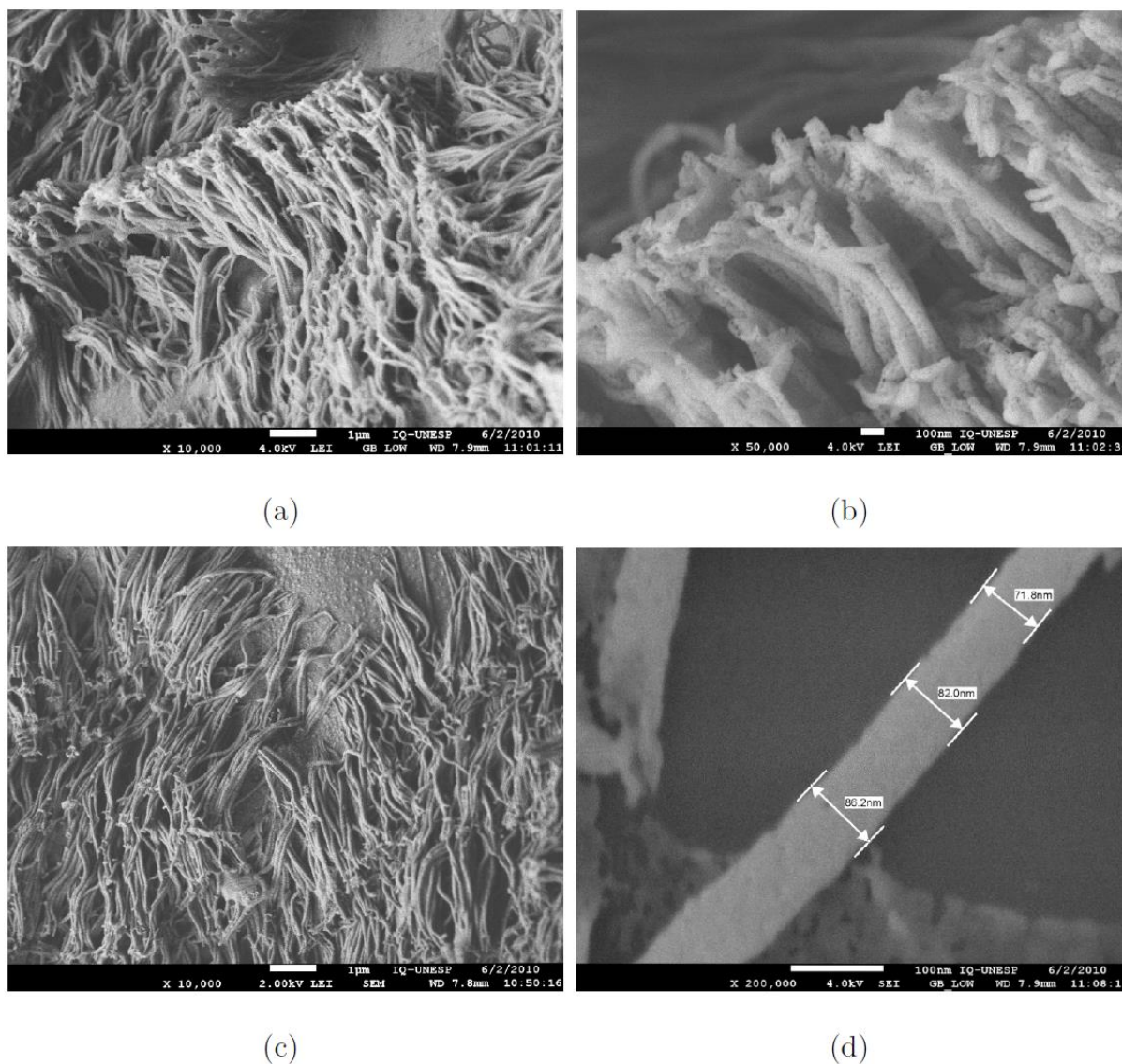


Figure 4. Detailed FEG-SEM micrograms of zirconium titanate nanowires.

ZrTiO_4 wires exhibit pore size of around 15 nm in diameter as a result of the incomplete densification process. This feature can enhance the sensing activity of the nanostructure, since the presence of pores in the nanowire increases the surface area [17]. Despite the incomplete densification and low temperature used in the preparation, the nanowire oxides present a homogeneous phase.

The membrane template-assisted methods require good wettability between the precursor solution and templates to ensure complete filling of

the membrane pores. If the precursor solution has good wettability with the template membrane, the capillary forces drive the solution into the pores [18]. The nanowire morphology shows that the chemical strategy adopted ensured the wettability of the polycarbonate membrane, since ZrTiO_4 nanowires grow by random diffusion of the oxide particles inside the polycarbonate membrane pores as a result of complete filling of the precursor solution before thermal treatment. The blockage of the membrane surface pores did not occur because the nanowires grew toward the direction of the free surface of the membrane. However, we can observe the formation of

films and ZrTiO_4 plates on the silicon substrate surface.

ZrTiO_4 nanowires grew by random diffusion of the oxide particles inside the polycarbonate membrane pores as the result of complete filling of the precursor solution. The nanowires' formation showed that the adopted chemical strategy ensured the wettability of the polycarbonate membrane.

In-situ chemical analysis was carried out on a single nanowire by EDS to confirm the oxide composition (Figure 5). According to the EDX profile, emission lines of zirconium, titanium, oxygen and silicon were detected, corroborating the composition of the ZrTiO_4 nanowire oxide identified in the XRD experiments.

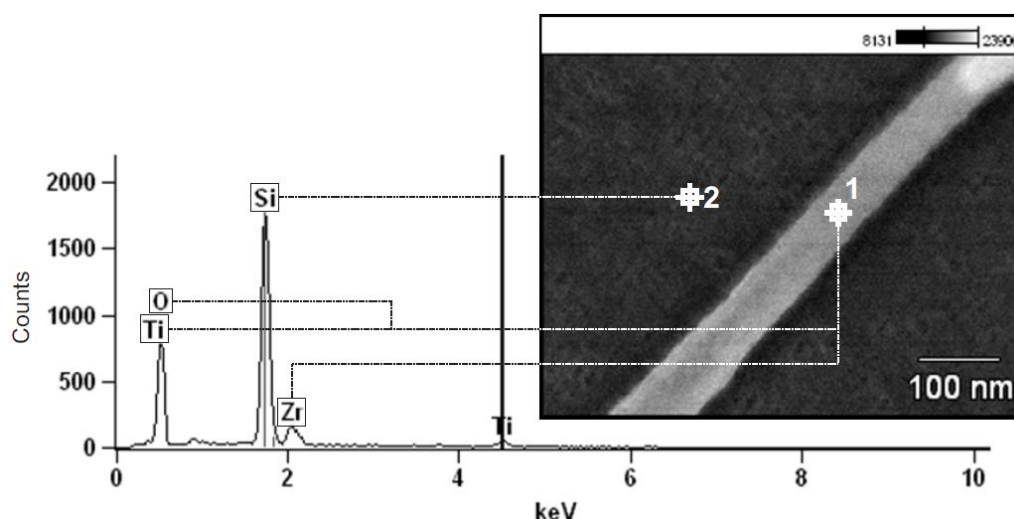


Figure 5. In-situ chemical analysis of the ZT-nws investigated by EDS. (1) ZrTiO_4 nanowire. (2) Silicon wafer.

Advantages of using PC as the template are its ease of handling and easy removal by means of pyrolysis, but its flexibility makes it prone to distortion during the heating process. In the formation of an oxide nanostructure, the removal of the template can occur before the start of densification [18]. Polycarbonate membranes start to soften at approximately 150 °C and melt at around 240 °C. The low thermal template stability could restrain the oxide nanostructure growth during annealing of the precursor solution due to the destruction of the porous structure of the template. By using the membrane-assisted Pechini route this event was avoided due to the formation of a characteristic glassy organic precursor at temperatures below 200 °C, which anchors the oxide structure inside the pores before the collapse of the porous membrane. In addition, the smooth surface of the silicon substrate contributed significantly to maintaining the pore structure during the thermal treatment and to the formation of the ZT-nws.

4. CONCLUSION

This membrane-assisted synthesis associated

with the polymeric precursor method was used in the first reported synthesis of ZrTiO_4 nanowires with controlled chemical compositions and high aspect ratio on a silicon substrate. The wires exhibit a pore formation because the incomplete densification process. This approach could potentially be extended in the future to process many other functional multi-component oxides as 1D nanostructures.

5. ACKNOWLEDGMENTS

The authors gratefully acknowledge the financial support of the Brazilian research funding institutions CNPq (process number: 550379/2007-0), through the national nanotechnology program, CAPES and FAPESP.

6. REFERENCES AND NOTES

- [1] Nikoobakht, B. *Chem. Mater.*, **2007**, *19*, 5279. [\[CrossRef\]](#)
- [2] Shaalan, N. M.; Yamazaki, T.; Kikuta, T. *Mater. Chem. Phys.* **2011**, *127*, 143. [\[CrossRef\]](#)
- [3] Law, M.; Goldberger, J.; Yang, P. *Annu. Rev. Mater. Res.* **2004**, *34*, 122. [\[CrossRef\]](#)
- [4] Melghit, K.; Al-belushi, M. *Mater. Lett.* **2008**, *62*, 3358.

- [5] Fan, Z.; Ho, J. C.; Takahashi, T.; Yerushalmi, R.; Takeia, K.; Ford, A.C.; Chueh, Y.-L.; Javey, A. *Adv. Mater.* **2009**, *21*, 3730. [\[CrossRef\]](#)
- [6] Byun, J.; Lee, J. I.; Kwon, S.; Jeon, G.; Kim, J. K. *Adv. Mater.* **2010**, *22*, 2028. [\[CrossRef\]](#)
- [7] Wang, X.W.; Yuan, Z. H.; Fang, B. C. *Mater. Chem. Phys.* **2011**, *125*, 1. [\[CrossRef\]](#)
- [8] De Lucena, P. R.; Pessoa-Neto, O. D.; Santos, I. M. G.; Souza, A. G.; Longo, E. *J. Alloy. Compd.* **2005**, *397*, 255. [\[CrossRef\]](#)
- [9] Martin, C.; *Science* **1994**, *266*, 1961. [\[CrossRef\]](#)
- [10] Hultheen, J.; Martin, C. *J. Mater. Chem.* **1997**, *7*, 1075. [\[CrossRef\]](#)
- [11] Choi, Y.; Kim, J.; Bu, S. *Mat. Sci. Eng. B-Solid*, **2006**, *133*, 245. [\[CrossRef\]](#)
- [12] Watanabe, H.; Kunitake, T. *Chem. Mater.*, **2008**, *20*, 4998. [\[CrossRef\]](#)
- [13] Kim, J.; Yang, S. A.; Choi, Y. C.; Han, J. K.; Jeong, K. O.; Yun, Y. J.; Yang, D. J. K.S. M.; Yoon, D.; Cheong, H.; Chang, K.-S.; Noh, T.W.; Bu, S. D. *Nanoletters* **2008**, *8*, 1813. [\[CrossRef\]](#)
- [14] Hua, Z.; Yang, P.; Huang, H.; Wan, J.; Yu, Z.-Z.; Yang, S.; Lu, M.; Gu, B.; Du, Y. *Mater. Chem. Phys.* **2008**, *107*, 541. [\[CrossRef\]](#)
- [15] Chung, Y.-A.; Lee, C.-Y.; Peng, C.-W.; Chiu, H.-T. *Mater. Chem. Phys.* **2006**, *100*, 380. [\[CrossRef\]](#)
- [16] De Lucena, P. R., Leite, E.; Pontes, F.; Longo, E.; Pizani, P.; Varela, J. *J. Solid State Chem.* **2006**, *179*, 3997. [\[CrossRef\]](#)
- [17] Kolmakov, A.; Moskovits, M. *Annu. Rev. Mater. Res.* **2004**, *34*, 151. [\[CrossRef\]](#)
- [18] Cao, G.; Liu, D. *Adv. Colloid Interfac.* **2008**, *136*, 45. [\[CrossRef\]](#)